Microchimica Acta
https://doi.org/10.1007/s00604-019-3421-x

ORIGINAL PAPER

Voltammetric sensing performances of a carbon ionic liquid electrode modified with black phosphorene and hemin

Xiaoyan Li[1] · Guiling Luo[1] · Hui Xie[1] · Yanyan Niu[1] · Xiaobao Li[1] · Ruyi Zou[1] · Yaru Xi[1] · Yi Xiong[1] · Wei Sun[1] · Guangjiu Li[2]

Received: 27 November 2018 / Accepted: 8 April 2019

Abstract

A black phosphorene (BPE) and poly(3,4-ethylenedioxythiophene)-poly(styrenesulfonate) (PEDOT:PSS) hybrid was used for the immobilization of hemin on a carbon ionic liquid electrode (CILE). BPE inside the PEDOT:PSS film was stable without adverse effects of water and oxygen. The hemin-modified electrode facilitates electrochemical communication with a couple of well-shaped and enhanced redox waves. Therefore BPE exhibits an accelerating function to the electron movement. This sensor exhibits excellent electrocatalytic effects on the reduction of various substrates including trichloroacetic acid (TCA), nitrite and H_2O_2. As for TCA, the reduction current at −0.36 V (vs. Ag/AgCl) increases linearly in the concentration range from 2.0 to 180 mmol·L^{-1} with a detection limit of 0.67 mmol·L^{-1} (at 3σ). As for nitrite, the reduction current at −0.59 Vis linear in the 1.0 to 10.5 mmol·L^{-1} concentration range, and the detection limit is 0.33 mmol·L^{-1} (at 3σ). As for H_2O_2, the reduction current at −0.033 V (vs. Ag/AgCl) is linear in the concentration range from 4.0 to 35.0 mmol·L^{-1} and the detection limit is 1.3 mmol·L^{-1} (at 3σ). The real sample was analyzed with satisfactory results, which indicated that BPE had potential applications in the field of electrochemical biosensor.

Keywords Black phosphorene · Hemin · Electrochemical biosensor · Electrocatalytic effect · Poly(3,4-ethylenedioxythiophene)-poly(styrenesulfonate) · Carbon ionic liquid electrode · Direct electrochemistry · Trichloroacetic acid · Nitrite · Hydrogen peroxide

Introduction

Layered nanomaterials are composed of single layer that exhibit many unique properties such as large specific surface area, good conductivity and so on. As a new emerging two-dimensional (2D) nanomaterial, black phosphorus (BP) attracts great interest. BP has layered structure and semiconductor properties [1], which has been used in high-performance electrochemical devices [2], optoelectronic [3] and medicine [4] due to novel electronic structures and optoelectronic properties. Also BP has tunability, highly mobility value with wide range of direct bandgap, which is superior to other atomically and ultra-thin layered nanomaterials including graphene [5], boron nitride [6] or transition metal dichalcogenides [7]. However, many researches about BP show that it is unstable in ambient conditions and easily degraded by reaction with water and oxygen in air, which lead to the degradation of the device performance [8] and seriously hinder the real application of BP. Various effective methods including the operation of preparing BP device in vacuum or inert environment, or the minimized exposing time in air can be used to protect BP from degradation. Wood et al. encapsulated BP by alumina film to lessen BP degradation in air/moisture [9]. Avsar et al. sealed BP by using graphene as the source leakage electrode and hexagonal boron nitride as the encapsulation layer in the inert gas condition [10]. In order to protect BP and reduce the degradation rate, another common

✉ Wei Sun
swyy26@hotmail.com

[1] Key Laboratory of Laser Technology and Optoelectronic Functional Materials of Hainan Province, Key Laboratory of Functional Materials and Photoelectrochemistry of Haikou, College of Chemistry and Chemical Engineering, Hainan Normal University, Haikou 571158, People's Republic of China

[2] Key Laboratory of Optic-electric Sensing and Analytical Chemistry for Life Science of Ministry of Education, College of Chemistry and Molecular Engineering, Qingdao University of Science and Technology, Qingdao 266042, People's Republic of China

Published online: 26 April 2019

and effective strategy is to cover the BP surface with a protective film. It has been reported that poly(3,4-ethylenedioxythiophene)-poly(styrenesulfonate) (PEDOT:PSS) can protect BP. Poly(3,4-ethylenedioxythiophene) (PEDOT) is an effective organic electronic material with the characteristics such as low oxidation potential, moderate band gap and inherent stability. It can dopant with poly(styrene sulfonic acid) (PSS) during polymerization to get a composite (PEDOT:PSS), which has good film forming properties and excellent stability [11]. Xu et al. prepared a soluble nanocomposite (PEDOT:PSS/Au) and used it as biomaterial for HRP immobilization to design HRP/PEDOT:PSS/Au modified electrode [12]. Lee et al. confirmed that the presence of BP in PEDOT:PSS increased conductivity with good stability [13]. Harano et al. showed that PEDOT:PSS promoted heterogeneous nucleation of crystallization and aggregation of donor materials with the formation of a flat and uniform film on the surface [14]. Our group also used PEDOT:PSS and black phosphorene (BPE) composite to construct electrochemical sensors for rutin and hemoglobin (Hb) investigation [15, 16].

Here in, an electrochemical biosensor was designed with BPE and hemin as electrode modifiers, which was mixed with PEDOT:PSS to get a stable film on the electrode. Hemin is a synthetic porphyrin molecule with π conjugated structure, which has a catalytic center with structure similar to redox proteins such as cytochrome C, peroxidase and Hb [17, 18]. Ranjani et al. constructed a sensing platform for the amperometric analysis of nitrite by titanium dioxide nanotubes and hemin modified glassy carbon electrode [19]. Hemin is also a good electronic medium and has good electrocatalytic activity for redox reaction of small molecules. Carbon ionic liquid electrode (CILE) belongs to carbon paste electrode that prepared by ionic liquid and graphite powder with the advantages including high conductivity, good anti-pollution ability, excellent detection sensitivity and specific electrocatalytic behavior, which has been applied in electrochemical sensor [20, 21]. By exploring CILE as the substrate electrode, an electrochemical sensor using BPE and hemin modified CILE was designed with excellent performance, which highly extended the usage of BPE in the development of biosensors.

Experimental

Reagents and apparatus

Hemin chloride (Hefei Bomei Biotechnology Co., China, http://www.bomei.bioon.com), BPE nanosheets (Nanjing XFNANO Mater. Co., China, https://www.xfnano.com), 1-hexylpyridinium hexafluorophosphate ($HPPF_6$, Lanzhou Yulu Fine Chem. Co., China, http://www.ilssale.com), PEDOT:PSS (Kuer Chem. Tech. Co., China, http://www.kuerhuaxue.com), graphite powder (average particle size 30 μm, Shanghai Colloid Chem. Co., China, https://shjthg.cn.china.cn), TCA (Tianjin Kemiou Chem. Co., China, http://www.chemreagent.com), $NaNO_2$ (Sinopharm Chemical Reagent Co. Ltd., Shanghai, China, http://5716366.1024sj.com) and H_2O_2 (Xilong Scientific Co. Ltd., China, http://www.xlhg.com) were used as received. All solutions were prepared by doubly distilled water and other chemical reagents used were of analytical grade.

A CHI 1220B electrochemical workstation (Shanghai CH Instrument, China, http://www.chinstr.com) was applied to all voltammetric experiments using a traditional three-electrode cell, which was consisted of a hemin based working electrode (Φ = 4 mm), a platinum wire counter electrode and an Ag/AgCl (3.0 mol·L^{-1} KCl) reference electrode.

Electrode fabrication

The stepwise fabrication of the electrochemical sensor was shown in Scheme 1. Firstly, CILE was fabricated by using the mixture of graphite powder and ionic liquid $HPPF_6$ (mass ratio of 2:1), which was put tightly in glass electrode tube (Φ = 4 mm) and connected by a copper wire. Then CILE was used as the substrate electrode with its surface polished to mirror-like before use [22]. Inside the nitrogen-filled glovebox, BPE nanosheets and PEDOT:PSS were mixed by a weight ratio of 1:5, and a uniform BPE-PEDOT:PSS mixture was obtained by ultra-sonication for 3 h. The mixture was further blended with 30.0 mg·mL^{-1} hemin solution by vibrating, and 8.0 μL solution was dropcasted onto CILE and dried in glovebox with the N_2 atmosphere to obtain BPE-PEDOT:PSS-hemin/CILE. For comparison, various modified electrodes such as BPE-PEDOT:PSS/CILE, PEDOT:PSS/CILE and PEDOT:PSS-hemin/CILE were fabricated by the similar procedures in the N_2 filled glovebox. Then electrochemistry of hemin modified electrode was studied by cyclic voltammetry with electrocatalysis to different targets investigated carefully.

Results and discussion

Electrochemical investigations

As shown in Fig. 1a, no redox peaks were found at BPE-PEDOT:PSS/CILE (curve a) and PEDOT:PSS/CILE (curve b) in a 0.1 mol·L^{-1} pH 2.0 phosphate buffered solution, indicating electroinactive material present on the electrode. Direct electrochemistry of hemin on different electrodes was measured with cyclic voltammograms present in Fig. 1b. A couple of asymmetric redox peaks was observed on PEDOT:PSS-hemin/CILE (curve c) and BPE-PEDOT:PSS-hemin/CILE (curve d), indicating that electrode reaction of hemin was

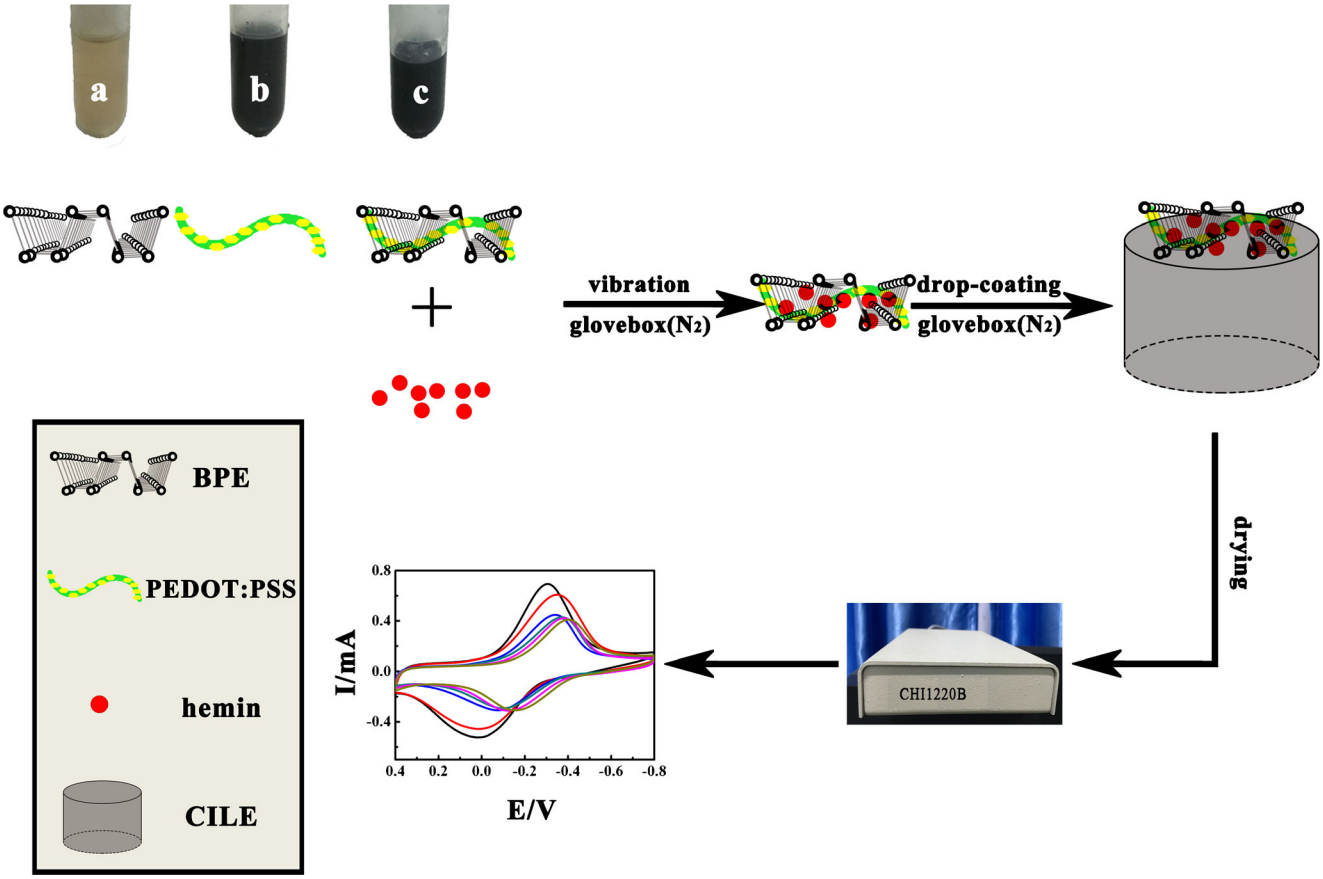

Scheme 1 Photos of (**a**) BPE solution, (**b**) PEDOT:PSS, (**c**) BPE-PEDOT:PSS (1:5) dispersion, and the fabrication procedure of this electrochemical biosensor

realized [23]. As a conductive polymer, PEDOT:PSS is benefit for the electron transfer of hemin on electrode with high stability. Due to its metalloporphyrin structure, hemin is often acted as media with the reversible reaction of Fe(III)/Fe(II) redox couple. The redox responses of hemin were enhanced after the incorporation of BPE nanosheets, which indicated that BPE had the positive effects to direct electron transfer of hemin. As shown in reference [16], electrochemical responses of this hemin modified electrode were larger than that of Hb modified electrode with the same BPE-PEDOT:PSS composite. The reason maybe the deeply buried of the same electroactive center inside the dense polypeptide layers of Hb that hinder the electron transfer rate. As a p-type semiconductive nanosheet, BPE can interact with PEDOT:PSS by non-covalent to result a stable hybrid with the conductivity enhanced. Also BPE has unique 2D layer structure with high carrier mobility and big surface area that have effective contact and electron transfer with hemin. Zhang et al. reported the stability investigation of BP with PEDOT:PSS, which was not influenced by oxygen and water [24]. Therefore, BPE could be protected by PEDOT:PSS and used as the modifier on the CILE. The peak currents of BPE-PEDOT:PSS-hemin/CILE are about 1.2-fold higher than those on PEDOT:PSS-hemin/CILE, indicating BPE on the modified electrode further enhances the electron transfer from hemin to electrode.

The buffer pH influenced the redox reaction of hemin with cyclic voltammograms recorded at pH ranged from 2.0 to 7.0. As shown in Fig. 1c and d, the maximum electrochemical response of this biosensor was attained at pH 2.0 phosphate buffered solution, which was chosen as the optimal supporting electrolyte. The redox peak potentials moved negatively with increasing pH. The formal peak potential ($E^{0'}$) has a good linearity with pH value, and the equation is $E^{0'}(V) = -0.0427$ pH - 0.0445 ($\gamma = 0.999$), proving protons take part in the reaction.

Electrochemical behaviors of BPE-PEDOT:PSS-hemin/CILE were recorded by varying scan rate and the results were shown in Fig. 1e. Both the anodic and cathodic peak currents increase with scan rate from 100 to 800 $mV{\cdot}s^{-1}$, inferring a surface-controlled electrode process. Linear relationships between redox peak potential (Ep) and lnυ were also constructed and the following Laviron's equation was used to calculate the electrochemical parameters [25]:

$$E_{pa} = E^{0'} + \frac{RT}{(1-\alpha)nF}\ln\upsilon \quad (1)$$

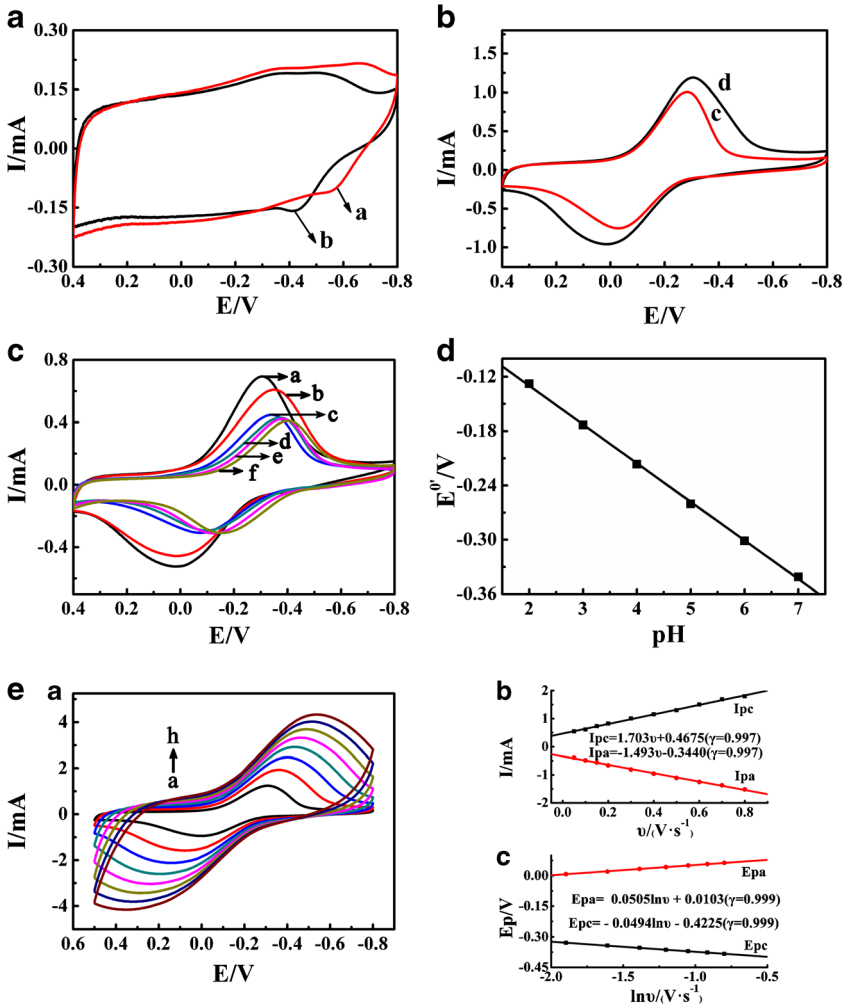

Fig. 1 Cyclic voltammograms of (**a**) BPE-PEDOT:PSS/CILE (a) and PEDOT:PSS/CILE (b), (**b**) PEDOT:PSS-hemin/CILE (c) and BPE-PEDOT:PSS-hemin/CILE (d) in 0.1 mol·L^{-1} pH 2.0 phosphate buffered solution at 100 mV·s^{-1}; (**c**) Cyclic voltammograms of BPE-PEDOT:PSS-hemin/CILE at different pH phosphate buffered solution (a to f represent 2.0, 3.0, 4.0, 5.0, 6.0, 7.0) at 100 mV·s^{-1}; (**d**) Relationship of $E^{0'}$ with pH; (**e**) (a) Effect of scan rate on redox responses of BPE-PEDOT:PSS-hemin/CILE in pH 2.0 phosphate buffered solution (a to h represent 100, 200, 300, 400, 500, 600, 700, 800 mV·s^{-1}), (b) Relationship of Ip with υ and (c) relationship of Ep with ln υ

$$E_{pc} = E^{0'} - \frac{RT}{\alpha nF}\ln\upsilon \quad (2)$$

$$\log k_s = \alpha\log(1-\alpha) + (1-\alpha)\log\alpha - \log\frac{RT}{nF\upsilon} - (1-\alpha)\alpha\frac{nF\Delta E_p}{2.3RT} \quad (3)$$

Then electron transfer number (n), the charge transfer coefficient (α) and the apparent heterogeneous electron transfer rate constant (k_s) are obtained to be 1.03, 0.53 and 1.58 s^{-1}. According to the equation $\Gamma^* = Q/nAF$ for the calculation of surface electroactive concentration (Γ^*), where Q corresponds to the quantity of electricity, n represents electron transfer number, F is the Faraday's constant and A is for geometric area [26]. The value of Γ^* is calculated as 8.62×10^{-6} mol·cm^{-2}. The total concentration of hemin on the modified electrode surface is 1.46×10^{-4} mol·cm^{-2}, so 5.88% of hemin is involved in electrochemical reaction. Therefore the layered 2D BPE with the large surface area can absorb more hemin through π-π stacking interactions on its surface, and electron transfer from the electroactive center is easily realized with electrochemical response enhanced.

Electrocatalytic properties

Because of the same catalytic active centre of hemin with peroxidase, it has been reported that hemin exhibits good electrocatalysis to many small molecules such as nitrite [27], serotonic [28] and hydrogen peroxide [29]. Therefore, electrocatalytic properties of BPE-PEDOT:PSS-hemin/CILE to various substrates were checked in detail due to the excellent biocatalytic activity of hemin.

Trichloroacetic acid (TCA) is an organic halide with potential environmental damage, therefore it is essential to find a reliable and sensitive procedure for TCA analysis [30]. As illustrated in Fig. 2a, electrocatalytic performance of BPE-PEDOT:PSS-hemin/CILE to TCA was recorded in pH 2.0 phosphate buffered solution. The reduction peak at −0.359 V (vs. Ag/AgCl) increases with TCA concentration and the oxidation current in cyclic voltammogram decreases. This indicates that the presence of hemin exhibits the catalytic effects to TCA reduction. The catalytic current increases linearly with TCA concentration from 2.0 to 180.0 mmol·L^{-1} (Fig. 2b) and the regression equation is I_{ss} (mA) = 0.015C

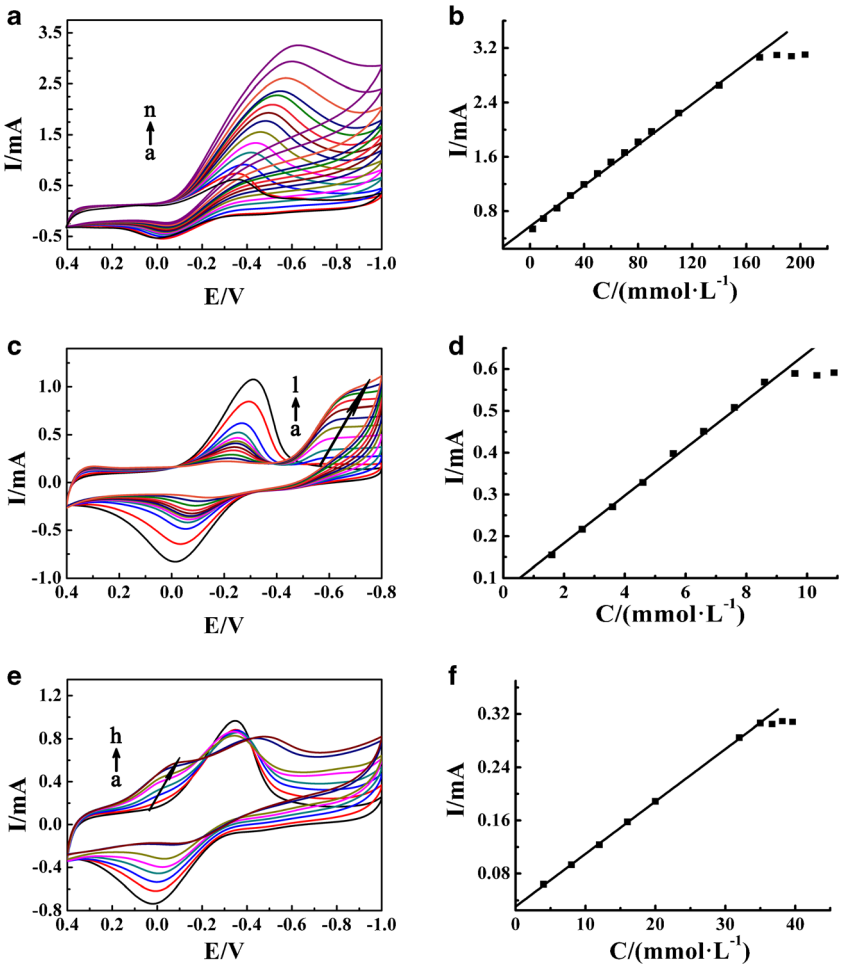

Fig. 2 Cyclic voltammograms of BPE-PEDOT:PSS-hemin/CILE in 0.1 mol·L^{-1} pH 2.0 phosphate buffered solution (**a**) with increasing trichloroacetic acid concentrations (curve a to n was 0, 2.0, 10.0, 20.0, 30.0, 40.0, 50.0, 60.0, 70.0, 80.0, 90.0, 110.0, 140.0, 170.0 mmol·L^{-1}), (**c**) with increasing nitrite concentrations (curve a to l was 0, 0.5, 1.0, 1.6, 2.6, 3.6, 4.6, 5.6, 6.6, 7.6, 8.6, 9.6 mmol·L^{-1}), (**e**) with increasing H_2O_2 concentrations (curve a to h was 0, 4.0, 8.0, 12.0, 16.0, 20.0, 32.0, 35.0 mmol·L^{-1}); Calibration plot of electrocatalytic current and the concentration of (**b**) TCA, (**d**) nitrite, (**f**) H_2O_2

(mmol·L^{-1}) + 0.58 ($\gamma = 0.997$) with the detection limit of 0.67 mmol·L^{-1} (3σ). After the TCA concentration exceeds 180.0 mmol·L^{-1}, the catalytic current becomes stable, proving a saturation reaction with a typical characteristic of the Michaelis-Menten kinetic process [31]. Based on the electrochemical format of Michaelis-Menten dynamic equation, the Michaelis-Menten constant (K_M^{app}) is obtained as 4.31 mmol·L^{-1} with the Lineweaver-Burk equation [32].

As nitrite has been utilized extensively in industry and meat processing, a fast and sensitive detection method for nitrite is necessary to be developed. Electrocatalytic behavior of BPE-PEDOT:PSS-hemin/CILE towards nitrite was measured with cyclic voltammograms illustrated in Fig. 2c. With the continuously addition of NO_2^-, the enhancement of the new reduction current at −0.592 V (vs. Ag/AgCl) and the disappearance of the original waves were observed, clearly proving an electrocatalytic behavior. The catalytic current has an excellent linear relationship with nitrite concentration from 1.0 to 10.5 mmol·L^{-1} (Fig. 2d). The linear regression equation is I_{ss} (mA) = 0.057C (mmol·L^{-1}) + 0.070 ($\gamma = 0.993$) with the detection limit estimated as 0.33 mmol·L^{-1} (3σ). After nitrite concentration is bigger than 10.5 mmol·L^{-1}, the catalytic current almost stays unchange, demonstrating a Michaelis-Menten dynamic mechanism and K_M^{app} is estimated to be 23.31 mmol·L^{-1}.

Also electrocatalytic reduction activity towards H_2O_2 was explored with cyclic voltammograms provided in Fig. 2e. The addition of H_2O_2 in buffer solution lead to a new reduction peak at −0.033 V (vs. Ag/AgCl) and a good linear relationship of H_2O_2 concentration with the catalytic currents is

Table 1 Analysis of TCA in medical facial peel solutions ($n = 3$)

	Detected (mmol·L^{-1})	Added (mmol·L^{-1})	Total (mmol·L^{-1})	Recovery (%)	RSD (%)
Medical facial peel solution (35% TCA)	146.33 ± 0.09	10.00	156.3 ± 0.1	99.9	1.11
		20.00	166.9 ± 0.2	100.4	1.42
		30.00	178.0 ± 0.3	101.1	2.51

Table 2 Comparison of analytical performances of various modified electrodes

Modified electrode	Analyte	Linear range (mmol·L^{-1})	LOD (mmol·L^{-1})	Refs
CTS/ELDH-GR-Hb/CILE	TCA	5.0–360.0	1.50	[33]
CTS/CMS-Hb/CILE	TCA	2.0–70.0	0.30	[34]
HA-HRP-CdS-IL/CILE	TCA	1.6~18.0	0.53	[35]
Nafion/nano-CdS/Hb/CILE	TCA	14.0–46.0	10.0	[36]
CTS-Mb-GR-IL/CILE	TCA	2.0~16.0	0.58	[37]
Nafion/HRP/Co_3O_4/CILE	TCA	5.0~90.0	1.7	[38]
	$NaNO_2$	0.1~1.1	0.033	
Nafion-Mb-SGO-GCE	$NaNO_2$	2.0~24.5	1.5	[39]
Nafion/Hb/B-GQDs/CILE	H_2O_2	4.0~24.0	1.3	[40]
Nafion/Mb/TiO_2@CNF/CILE	TCA	5.0~105.0	1.6	
	$NaNO_2$	1.0~70.0	0.3	[41]
	H_2O_2	2.8~32.0	1.0	
BPE-PEDOT:PSS-hemin/CILE	TCA	2.0~180.0	0.67	
	$NaNO_2$	1.0~10.5	0.33	This work
	H_2O_2	4.0~35.0	1.33	

*CTS: chitosan; ELDH: exfoliated Co_2Al layered double hydroxide; GR: graphene; Hb: hemoglobin; CMS: carbon microspheres; HA: hyaluronic acid; HRP: horseradish peroxidase; CdS: cadmium sulfide; Mb: myoglobin; SGO: sulfonated graphene oxide; GCE: glassy carbon electrode; B-GQDs: boron-doped graphene quantum dots; TiO_2@CNF: TiO_2-doped carbon nanofiber

established from 4.0 to 35.0 mmol·L^{-1} (Fig. 2f). The linear regression equation is I_{ss} (mA) = 0.0079C (mmol·L^{-1}) + 0.031 (γ = 0.998) with the detection limit and K_M^{app} obtained as 1.33 mmol·L^{-1} (3σ) and 11.85 mmol·L^{-1}.

Sample analysis and analyte detection

Medical facial peel solution (35% TCA, Shanghai EKEAR Biotech. Co., China) was detected by this hemin modified electrode with the result listed in Table 1 and the recovery was calculated by standard addition method. A satisfactory result is obtained with recoveries from 99.9% to 101.1%, validating the practicability of this biosensor in real sample.

Stability and reproducibility

The stability and reproducibility of this designed biosensor were examined by multi-scan cyclic voltammetry. The result shows that the current response of BPE-PEDOT:PSS-hemin/CILE decreases for 7.8% after 70 cycles in phosphate buffered solution (pH 2.0) and the current response retains 92.2% of the original sensitivity after storing for 15 days at 4 °C, indicating BPE-PEDOT:PSS-hemin/CILE has a good stability. Therefore, the long service life of BPE-PEDOT:PSS-hemin/CILE may be attributed to the fact that BPE-PEDOT:PSS composite is a suitable material with good biocompatibility and stability due to the protection of PEDOT:PSS to biocompatible phosphorene.

Conclusion

In this paper BPE nanosheets and hemin are chosen as the electrode modifier using PEDOT:PSS as protective film. Direct electrochemistry of hemin is realized with BPE as the enhancer and electrocatalysis of this modified electrode is checked. A systematic comparison with different redox protein/enzyme modified electrodes for the electrocatalytic detection of various substrates was listed in Table 2. Real sample is also analyzed with satisfactory result and this investigation effectively broaden the usage of BPE in electrochemical biosensor due to the high stability of BPE-PEDOT:PSS composite on the electrode.

Acknowledgments This work was financially supported by the National Natural Science Foundation of Hainan Province of China (2017CXTD007), the National Natural Science Foundation of China (21665007), the Program for Innovative Research Team in University (IRT-16R19), Research Fund from Beijing Innovation Center for Future Chips (KYJJ2018006), and the Key Science and Technology Program of Haikou City (2017042).

Compliance with ethical standards The author(s) declare that they have no competing interests.

References

1. Wang H, Yang XZ, Shao W, Chen SC, Xie JF, Zhang XD, Wang J, Xie Y (2015) Ultrathin black phosphorus nanosheets for efficient singlet oxygen generation. J Am Chem Soc 137:11376–11382
2. Pang JB, Bachmatiuk A, Yin Y, Trzebicka B, Zhao L, Fu L, Mendes RG, Gemming T, Liu ZF, Rummeli MH (2017) Applications of phosphorene and black phosphorus in energy conversion and storage devices. Adv Energy Mater 1702093:1–43
3. Sun ZY, Zhang YQ, Yu H, Yan C, Liu YC, Hong S, Tao HC, Robertson AW, Wang Z, Pádua AAH (2018) New solvent-stabilized few-layer black phosphorus for antibacterial applications. Nanoscale 10:12543–12553
4. Xiang Y, Xia QL, Luo JH, Liu YP, Peng YD, Wang DW, Nie YZ, Guo GH (2018) Observation of ferromagnetism in black phosphorus nanosheets with high magnetization by liquid exfoliation. Solid State Commun 281:1–5
5. Wu YQ, Lin YM, Bol AA, Jenkins KA, Xia FN, Farmer DB, Zhu Y, Avouris P (2011) High-frequency, scaled graphene transistors on diamond-like carbon. Nature 472:74–78
6. Feng CP, Bai L, Bao RY, Liu ZY, Yang MB, Chen J, Yang W (2018) Electrically insulating POE/BN elastomeric composites with high through-plane thermal conductivity fabricated by two-roll milling and hot compression. Adv Compos Hybrid Mater 1:160–167
7. Das S, Chen HY, Penumatcha AV, Appenzeller J (2013) High performance multilayer MoS_2 transistors with scandium contacts. Nano Lett 13:100–105
8. Island JO, Steele GA, van der ZHSJ, Castellanos-Gomez A (2015) Environmental instability of few-layer black phosphorus. 2D Mater 2:011002
9. Wood JD, Wells SA, Jariwala D, Chen KS, Cho E, Sangwan VK, Liu XL, Lauhon LJ, Marks TJ, Hersam MC (2014) Effective passivation of exfoliated black phosphorus transistors against ambient degradation. Nano Lett 14:6964–6970
10. Avsar A, Vera-Marun IJ, Tan JY, Watanabe K, Taniguchi T, Castro Neto AH, Özyilmaz B (2015) Air-stable transport in graphene-contacted, fully encapsulated ultrathin black phosphorus-based field-effect transistors. ACS Nano 9:4138–4145
11. Groenendaal LB, Jonas F, Freitag D, Pielartzik H, Reynolds JR (2000) Poly(3,4-ethylenedioxythiophene) and its derivatives: past, present, and future. Adv Mater 12:481–494
12. Xu JJ, Peng R, Ran Q, Xian YZ, Tian Y, Jin LT (2010) A highly soluble poly(3,4-ethylenedioxythiophene)-poly(styrene sulfonic acid)/au nanocomposite for horseradish peroxidase immobilization and biosensing. Talanta 82:1511–1515
13. Lee JY, Lin YJ (2016) Effect of incorporation of black phosphorus into PEDOT:PSS on conductivity and electron-phonon coupling. Synthetic Met 212:180–185
14. Harano K, Okada S, Furukawa S, Tanaka H, Nakamura E (2014) Formation of a polycrystalline film of donor material on PEDOT:PSS buffer induced by crystal nucleation. J Polym Sci Pol Phys 52:833–841
15. Niu XL, Weng WJ, Yin CX, Niu YY, Li GJ, Dong RX, Men YL, Sun W (2018) Black phosphorene modified glassy carbon electrode for the sensitive voltammetric detection of rutin. J Electroanal Chem 811:78–83
16. Li XY, Niu XL, Zhao WS, Chen W, Yin CX, Men YL, Li GJ, Sun W (2018) Black phosphorene and PEDOT:PSS-modified electrode for electrochemistry of hemoglobin. Electrochem Commun 86:68–71
17. Shi F, Zheng WZ, Wang WC, Hou F, Lei BX, Sun ZF, Sun W (2015) Application of graphene-copper sulfide nanocomposite modified electrode for electrochemistry and electrocatalysis of hemoglobin. Biosens Bioelectron 64:131–137
18. Qian DP, Li WB, Chen FT, Huang Y, Bao N, Gu HY, Yu CM (2017) Voltammetric sensor for trichloroacetic acid using a glassy carbon electrode modified with au@ag nanorods and hemoglobin. Microchim Acta 184(7):1977–1985
19. Ranjani B, Kalaiyarasi J, Pavithra L, Devasena T, Pandian K, Gopinath SC (2018) Amperometric determination of nitrite using natural fibers as template for titanium dioxide nanotubes with immobilized hemin as electron transfer mediator. Microchim Acta 185(3):185–194
20. Wang XF, You Z, Cheng Y, Sha HL, Li GJ, Zhu HH, Sun W (2015) Application of nanosized gold and graphene modified carbon ionic liquid electrode for the sensitive electrochemical determination of folic acid. J Mol Liq 204:112–117
21. Sun W, Wang XL, Lu YX, Gong SX, Qi XW, Lei BX, Sun ZF, Li GJ (2015) Electrochemical deoxyribonucleic acid biosensor based on electrodeposited graphene and nickel oxide nanoparticle modified electrode for the detection of salmonella enteritidis gene sequence. Mat Sci Eng C-Mater 49:34–39
22. Zheng W, Chen W, Weng WJ, Liu L, Li GJ, Wang JW, Sun W (2017) Direct electron transfer of horseradish peroxidase at Co_3O_4-graphene nanocomposite modified electrode and electrocatalysis. J Iran Chem Soc 14:925–932
23. Guo CX, Hu FP, Li CM, Shen PK (2008) Direct electrochemistry of hemoglobin on carbonized titania nanotubes and its application in a sensitive reagentless hydrogen peroxide biosensor. Biosens Bioelectron 24:819–824
24. Zhang J, Ding WC, Zhang ZX, Xu JK, Wen YP (2016) Preparation of black phosphorus-PEDOT:PSS hybrid semiconductor composites with good film-forming properties and environmental stability in water containing oxygen. RSC Adv 6:76174–76182
25. Laviron E (1979) General expression of the linear potential sweep voltammogram in the case of diffusionless electrochemical systems. J Electroanal Chem 101:19–28
26. Bard AJ, Faulkner LR (1980) Electrochemical methods: fundamentals and applications. Wiley, New York
27. Mimica D, Zagal JH, Bedioui F (2001) Electroreduction of nitrite by hemin, myoglobin and hemoglobin in surfactant films. J Electroanal Chem 497:106–113
28. Santos WDJR, Lima PR, Tarley CRT, Höehr NF, Kubota LT (2009) Synthesis and application of a peroxidase-like molecularly imprinted polymer based on hemin for selective determination of serotonin in blood serum. Anal Chim Acta 631:170–176
29. Zhang Y, Xia Z, Liu H, Yang MJ, Lin LL, Li QZ (2013) Hemin-graphene oxide-pristine carbon nanotubes complexes with intrinsic peroxidase-like activity for the detection of H_2O_2 and simultaneous determination for Trp, AA, DA, and UA. Sens Actuator B 188:496–501
30. Bhat HK, Kanz MF, Campbell GA, Ansari GAS (1991) Ninety day toxicity study of chloroacetic acids in rats. Fundam Appl Toxicol 17:240–253
31. Wang WC, Li XQ, Yu XH, Yan LJ, Lei BX, Li P, Chen CX, Sun W (2016) Electrochemistry and electrocatalysis of myoglobin on electrodeposited ZrO_2 and graphene modified carbon ionic liquid electrode. J Iran Chem Soc 13:323–330
32. Li J, Tan SN, Ge HL (1996) Silica sol-gel immobilized amperometric biosensor for hydrogen peroxide. Anal Chim Acta 335:137–145
33. Zhan TR, Wang XJ, Li XJ, Song Y, Hou WG (2016) Hemoglobin immobilized in exfoliated Co2Al LDH-graphene nanocomposite film: direct electrochemistry and electrocatalysis toward trichloroacetic acid. Sensor Actuat B-Chem 228:101–108

34. Wang WC, Yan LJ, Shi F, Niu XL, Huang GL, Zheng CJ, Sun W (2016) Application of carbon-microsphere-modified electrodes for electrochemistry of hemoglobin and Electrocatalytic sensing of Trichloroacetic acid. Sensors 16:6
35. Zhu ZH, Li X, Wang Y, Zeng Y, Sun W, Huang XT (2010) Direct electrochemistry and electrocatalysis of horseradish peroxidase with hyaluronic acid-ionic liquid-cadmium sulfide nanorod composite material. Anal Chim Acta 670:51–56
36. Sun W, Wang DD, Li GC, Zhai ZQ, Zhao RJ, Jiao K (2008) Direct electron transfer of hemoglobin in a CdS nanorods and Nafion composite film on carbon ionic liquid electrode. Electrochim Acta 53:8217–8221
37. Ruan CX, Li TT, Niu QJ, Lu M, Lou J, Gao WM, Sun W (2012) Electrochemical myoglobin biosensor based on graphene-ionic liquid-chitosan bionanocomposites: direct electrochemistry and electrocatalysis. Electrochim Acta 64:183–189
38. Chen W, Weng WJ, Yin CX, Niu XL, Li GJ, Xie H, Liu J, Sun W (2018) Fabrication of an electrochemical biosensor based on Nafion/horseradish peroxidase/Co_3O_4 NP/CILE and its Electrocatalysis. Int J Electrochem Sci 13:4741–4752
39. Chen GY, Sun H, Hou SF (2016) Electrochemistry and electrocatalysis of myoglobin immobilized in sulfonated graphene oxide and Nafion films. Anal Biochem 502:43–49
40. Chen W, Weng WJ, Niu XL, Li XY, Men YL, Sun W, Li GJ, Dong LF (2018) Boron-doped graphene quantum dots modified electrode for electrochemistry and electrocatalysis of hemoglobin. J Electroanal Chem 823:137–145
41. Niu YY, Xie H, Luo GL, Weng WJ, Ruan CX, Li GJ, Sun W (2019) Electrochemical performance of myoglobin based on TiO_2-doped carbon nanofiber decorated electrode and its applications in biosensing. RSC Adv 9:4480–4487